

RESEARCH

Open Access



# Epithelial microRNA-30a-3p targets RUNX2/HMGB1 axis to suppress airway eosinophilic inflammation in asthma

Wenliang Wu<sup>1,2</sup>, Jiali Gao<sup>1,2</sup>, Dian Chen<sup>1,2</sup>, Gongqi Chen<sup>1,2</sup>, Yuchen Feng<sup>1,2</sup>, Chenli Chang<sup>1,2</sup>, Shengchong Chen<sup>1,2</sup>, Lingling Yi<sup>1,2\*</sup> and Guohua Zhen<sup>1,2\*</sup> 

## Abstract

**Background:** Type 2-high asthma is a prominent endotype of asthma which is characterized by airway eosinophilic inflammation. Airway epithelial cells play a critical role in the pathogenesis of asthma. Our previous miRNA profiling data showed that miR-30a-3p was downregulated in bronchial epithelial cells from asthma patients. We hypothesize that epithelial miR-30a-3p plays a role in asthma airway inflammation.

**Methods:** We measured miR-30a-3p expression in bronchial brushings of asthma patients (n = 51) and healthy controls (n = 16), and analyzed the correlations between miR-30a-3p expression and airway eosinophilia. We examined whether Runt-related transcription factor 2 (*RUNX2*) was a target of miR-30a-3p and whether *RUNX2* bound to the promoter of high mobility group box 1 (*HMGB1*) by using luciferase reporter assay and chromatin immunoprecipitation (ChIP)-PCR. The role of miR-30a-3p was also investigated in a murine model of allergic airway inflammation.

**Results:** We found that miR-30a-3p expression were significantly decreased in bronchial brushings of asthma patients compared to control subjects. Epithelial miR-30a-3p expression was negatively correlated with parameters reflecting airway eosinophilia including eosinophils in induced sputum and bronchial biopsies, and fraction of exhaled nitric oxide in asthma patients. We verified that *RUNX2* is a target of miR-30a-3p. Furthermore, *RUNX2* bound to the promoter of *HMGB1* and upregulated *HMGB1* expression. *RUNX2* and *HMGB1* expression was both enhanced in airway epithelium and was correlated with each other in asthma patients. Inhibition of miR-30a-3p enhanced *RUNX2* and *HMGB1* expression, and *RUNX2* overexpression upregulated *HMGB1* in BEAS-2B cells. Intriguingly, airway overexpression of mmu-miR-30a-3p suppressed *Runx2* and *Hmgb1* expression, and alleviated airway eosinophilia in a mouse model of allergic airway inflammation.

**Conclusions:** Epithelial miR-30a-3p could possibly target *RUNX2/HMGB1* axis to suppress airway eosinophilia in asthma.

**Keywords:** Epithelial cells, miR-30a-3p, Eosinophilia, *RUNX2*, *HMGB1*, Asthma

## Background

Asthma is a chronic airway disease characterized by airway hyperresponsiveness (AHR), airway inflammation, mucus overproduction, and submucosal fibrosis [1]. Type 2 immune response driven by the type 2 cytokines, IL-4, IL-5, and IL-13, plays an important role in the pathogenesis of asthma. The type 2-high and type 2-low asthma

\*Correspondence: yilingling20061281@163.com; ghzhen@tjh.tjmu.edu.cn

<sup>1</sup> Division of Respiratory and Critical Care Medicine, Department of Internal Medicine, Tongji Hospital, Tongji Medical College, Huazhong University of Science and Technology, Wuhan 430030, China, Full list of author information is available at the end of the article



endotypes are classified according to the expression levels of the type 2 cytokines [2]. Airway eosinophilic inflammation is a key feature of type 2-high asthma [3–6]. Airway epithelial cells contribute to airway eosinophilia by producing chemokines including C–C motif chemokine ligand (CCL)11, CCL24, and CCL26.

MicroRNAs (miRNAs) are ~22 nucleotide long, non-coding RNAs that play a critical role in the regulation of gene expression. MiRNAs have been implicated in the pathogenesis of asthma [7–9]. Significant alterations in miRNA expression of airway epithelial cells have been reported by us and others [10–12]. A recent study demonstrated that epithelial miR-141 regulates airway mucus production in asthma [7]. We previously reported that epithelial miRNAs were involved in asthmatic airway eosinophilia [10–12]. Our miRNA profiling data showed that a set of epithelial miRNAs including miR-30a-3p was downregulated in asthma patients [12]. MiR-30a-3p was reported to regulate the proliferation and apoptosis of cancer cells [13, 14]. A recent study showed that miR-30a-3p expression was significantly decreased in the peripheral blood of asthmatic patients [15]. However, the role of airway epithelial miR-30a-3p in the pathogenesis of asthma remains unclear. We hypothesized that epithelial miR-30a-3p is involved in airway eosinophilic inflammation in asthma.

Runt-related transcription factors (RUNXs) serve as key regulators in development and carcinogenesis [16–18]. There are three *RUNX* genes, *RUNX1*, *RUNX2* and *RUNX3*, in mammals. Maternal smoking could promote the development of asthma in the offspring by upregulating the expression of *RUNX1* [19]. *RUNX2* is reported to promote the gene transcription of SAM pointed domain containing ETS transcription factor (*SPDEF*), a key transcription factor in goblet cell differentiation [20]. A previous study suggests that *RUNX2* may bind to the promoter of high mobility group box 1 (*HMGB1*) [21].

*HMGB1* is a pro-inflammatory mediator belonging to the alarmin family [22]. *HMGB1* can interact with multiple surface receptors including toll-like receptors to promote inflammatory response [23]. It was reported that *HMGB1* enhanced the survival of eosinophils and served as a chemoattractant for eosinophils [24, 25]. *HMGB1* levels in induced sputum from asthmatic patients were elevated [26]. In animal models of asthma, airway eosinophilic inflammation was ameliorated by blocking *HMGB1* activity [26, 27]. These studies indicate that *HMGB1* contributes to airway eosinophilia in asthma.

In the present study, we found that downregulated epithelial miR-30a-3p expression was negatively correlated with airway eosinophilic inflammation in asthma patients. *RUNX2* was a target of miR-30a-3p, and *RUNX2* directly regulated *HMGB1* expression by

binding to the promoter of *HMGB1*. Epithelial *RUNX2* and *HMGB1* expression was both enhanced in asthma patients. In vitro, inhibition of miR-30a-3p expression promoted IL-13-induced *RUNX2* and *HMGB1* expression in airway epithelial cells. Intriguingly, airway overexpression of mmu-miR-30a-3p alleviated airway eosinophilia in a mouse model of allergic airway inflammation.

## Materials and methods

### Subjects

We recruited 16 control subjects and 51 patients with confirmed asthma who have obvious symptoms and. All subjects were recruited from Tongji Hospital. Asthma were diagnosed by a physician; had symptoms of episodic cough, wheeze and/or dyspnea; and had accumulated dosage of methacholine provoking a 20% fall ( $PD_{20}$ ) of forced expiratory volume in the first second ( $FEV_1$ ) < 2.505 mg and/or  $\geq 12\%$  increase in  $FEV_1$  following inhalation of 200  $\mu$ g salbutamol. Control subjects had no respiratory symptoms, normal spirometry value and methacholine  $PD_{20} \geq 2.505$  mg. None of the subjects had ever smoked or received inhaled or oral corticosteroid or leukotriene antagonist. Written informed consents were obtained from all subjects. The ethics committee of Tongji Hospital, Huazhong University of Science and Technology had approved the study.

For each subject, we recorded their demographic information, collected sputum specimens, and measured spirometry and fraction of exhaled nitric oxide (FeNO) at study entry. Bronchoscopy with brushing and endobronchial biopsies was performed within 1 week of study entry. Methods for histology and biopsy techniques, pulmonary function testing and FeNO measurement were described previously [28].

### Murine model of allergic airway inflammation

Six- to eight-week-old female C57BL/6J mice were sensitized with intraperitoneal injection of OVA solution (100  $\mu$ g in 100  $\mu$ L saline, Sigma-Aldrich, USA) mixed with  $Al(OH)_3$  as an adjuvant on days 0, 7 and 14. Mice were challenged with intranasal administration of OVA solution (1 mg in 50  $\mu$ L saline) on days 21, 22, 23, 24 and 25. Mmu-miR-30a-3p agomir (5 nmol in 40  $\mu$ L saline, RiboBio, China) or control agomir was administered intranasally 2 h before OVA challenge on days 21 and 23. Mice were sacrificed 24 h after the last OVA challenge. Lung tissues were collected for histological analysis and quantitative PCR. Animal experiments were approved by the ethics committee of Tongji Hospital, Huazhong University of Science and Technology.

### Assessment of airway inflammation

Cell counts for macrophages, eosinophils, lymphocytes, and neutrophils in bronchoalveolar lavage fluid (BALF) were performed. The severity of peribronchial inflammation in H&E-stained mouse lung sections was scored using the following features: 0, normal; 1, few cells; 2, a ring of inflammatory cells (1 cell layer deep); 3, a ring of inflammatory cells (2–4 cells deep); 4, a ring of inflammatory cells (> 4 cells deep) [29].

### Histology, immunohistochemistry and periodic acid-Schiff (PAS) staining

The human airway biopsy and mouse left lungs were paraffin-embedded, and 5- $\mu$ m sections were cut. Sections were used for hematoxylin and eosin (H&E) staining, periodic acid-Schiff (PAS) staining and immunohistochemical examination. For immunofluorescence staining, bronchial biopsy sections underwent antigen retrieval and were incubated with mouse monoclonal RUNX2 antibody (sc-390715 X, 1:1000 dilution, Santa Cruz Biotechnology, USA) and rabbit polyclonal HMGB1 antibody (10829-1-AP, 1:200 dilution, protein-tech, China), then incubated with Cy3 goat anti-mouse secondary antibody (ServiceBio, China) and FITC goat anti-rabbit secondary antibody (ServiceBio, China). Nuclei were stained with DAPI. Photographs were taken by using a fluorescence microscope (NIKON Eclipse ci, Japan). For PAS staining, lung sections were stained with PAS (Goodbio technology, China) for detection of mucus. The number of PAS-staining-positive cells was counted in 10 random fields for each lung section at  $\times 200$  magnification. Observers who were blinded to the clinical status of the subjects counted numbers of eosinophils/mm<sup>2</sup> submucosa as previously described [28].

### Cell culture and treatment

BEAS-2B cell lines were purchased from ATCC (Manassas, VA). Cells were cultured in DMEM medium (Gibco, USA) with 10% FBS (Biological Industries, Israel). Cells were stimulated with or without IL-13 (20 ng/mL, Peprotech, USA) and transfected with control or miR-30a-3p mimic (50  $\mu$ mol/L, RiboBio, China), control or miR-30a-3p inhibitor (100  $\mu$ mol/L, RiboBio, China), scrambled or RUNX2 siRNA (100  $\mu$ mol/L, RiboBio, China), and empty control or RUNX2 cDNA expression vector (500 ng/mL, GeneCopoeia, China) using Lipofectamine 3000 (Invitrogen, USA). The sequence of the sense strand of RUNX2 siRNA (5'-CTCTGCACCAAGTCCTTTTdT-3') have been described previously [21]. Forty-eight hours after IL-13

stimulation, cells were harvested for quantitative PCR and Western blotting. Cell culture medium was collected for ELISA.

### Quantitative PCR

Total RNA from human bronchial brushings, mouse lungs and BEAS-2B cells was isolated using TRIzol (Invitrogen, USA) and reversely transcribed to cDNA using PrimeScript RT reagent kit (Takara, Japan). The sequences of the primers for Sybr Green real-time PCR were obtained from PrimerBank. Other primer sequences were designed by Sangon Biotech, China. The transcript levels of 5 s, miR-30a-3p, *GUSB*, *RUNX2*, *HMGB1*, *Gapdh*, *Runx2*, *Hmgb1* and *Muc5ac* were determined by using Takara SYBR Premix ExTaq polymerase and a CFX Connect PCR System (Bio-Rad Laboratories, USA). Fold differences were determined by the  $2^{-\Delta\Delta CT}$  method [30]. The gene expression was expressed as log<sub>2</sub> transformed and relative to the median of control subjects or the mean of control group. The primers used are listed in Additional file 1: Table S2.

### Fluorescence in situ hybridization

We performed fluorescence in situ hybridization of hsa- and mmu-miR-30a-3p on paraffin-embedded sections using digoxin-labeled hsa- and mmu-miR-30a-3p miRNA probe (Qiagen, China). The sequence of the probes for both hsa- and mmu-miR-30a-3p was 5'-GCTGCAAACATCCGACTGAAAG-3'. The protocol was according to the manufacturer's instructions.

### Chromatin immunoprecipitation (ChIP) assay

ChIP assays were performed using a chromatin immunoprecipitation (ChIP) kit (#56383, Cell Signaling Technology, USA). BEAS-2B were treated with IL-13 (20 ng/mL, Biolegend, USA) for 48 h. Chromatin was sonicated to obtain 100–900-bp DNA/protein fragments after cells were cross-linked with formaldehyde. Then, anti-RUNX2 (rabbit mAb, D1L7E, Cell Signaling Technology, USA) or IgG were added to lysates and incubated at 4 °C overnight. The next day, ChIP-Grade Protein G Magnetic Beads were used for immunoprecipitation. Then DNA was released and purified for subsequent PCR and agarose gel electrophoresis. Standard PCR were performed to amplify human *HMGB1* promoter region containing the AAACCACAG sequence using the primers 5'-CGTGGTCTGCTCAGGCTAAA-3' (forward) and 5'-GCA TGTGCCCAAATCCACAG-3' (reverse).

### Luciferase activity assay

The vectors (pEZX-MT06, GeneCopoeia, USA) harboring wild-type, mutant *RUNX2* 3'-UTR or no 3'-UTR (control) were co-transfected with miR-30a-3p mimic or non-targeting control miRNA in BEAS-2B cells. After 24 h, cells were harvested and lysed and luciferase activity was measured with a Dual-Luciferase Reporter Assay Kit (Promega, USA). The firefly luciferase activity was normalized to renilla luciferase activity. To investigate whether *RUNX2* binds to the promoter of *HMGB1*, the wild type, truncated, or mutant *HMGB1* promoters were cloned into a pPro-RB-Report vector (RiboBio, China). These luciferase vectors were co-transfected with empty control or *RUNX2* cDNA expression vector in BEAS-2B cells. After 24 h, cells were harvested and luciferase activity was measured with a Dual-Luciferase Reporter Assay Kit (Promega, USA). The renilla luciferase activity was normalized to firefly luciferase activity.

### Western blotting

Proteins were extracted from BEAS-2B cells using RIPA buffer (Servicebio, China). Fifty micrograms of extracted proteins were separated using 10% SDS-PAGE, and the separated proteins were transferred onto polyvinylidene difluoride (PVDF) membranes (Roche, Germany). The membranes were first probed with indicated primary antibodies. Antibodies used in Western blot were: *RUNX2* (Abcam, ab23981, 1:1000 dilution), *HMGB1* (Proteintech, 10829-1-AP, 1:2000 dilution), *GAPDH* (Aspen, 1:2000 dilution). Then antibodies were detected using horseradish peroxidase-conjugated goat anti-rabbit IgG (Aspen, 1:4000 dilution) secondary antibody followed by ECL Western blot detection reagent (Med-ChemExpress, USA). Densitometry was assessed using ImageJ (National Institutes of Health, USA) and normalized to *GAPDH*.

### Enzyme linked immunosorbent assay (ELISA)

*HMGB1* protein levels in supernatant from BEAS-2B cell culture media and BALF of mouse was analyzed by ELISA (Shino-Test Corporation, Japan). ELISA was performed according to the manufacturer's instructions. All samples and standards were measured in duplicate.

### Statistical analysis

We analyzed data using Prism version 7.3 (GraphPad Software, San Diego, CA, USA). For normally distributed data, we calculated the means  $\pm$  standard deviation (SD) and used parametric tests (unpaired Student's *t* test or one-way analysis of variance with Tukey correction) to compare across groups. For non-normally distributed data, we calculated medians (with interquartile ranges)

**Table 1** Subjects characteristics

	Control subjects	Asthma patients	P value
Number	16	51	
Age, year	38.19 $\pm$ 6.48	39.22 $\pm$ 12.56	0.759
Sex, M:F (%F)	8:8 (50)	15:36 (70.1)	0.13
Body mass index	22.08 $\pm$ 2.49	22.09 $\pm$ 2.65	0.99
FEV <sub>1</sub> , % predicted	99.70 $\pm$ 8.85	80.27 $\pm$ 17.24	0.0003
Methacholine PD <sub>20</sub> , mg	2.505 $\pm$ 0	0.14 $\pm$ 0.24	< 0.0001
Sputum eosinophil, %	0.45 $\pm$ 0.55	16.01 $\pm$ 17.67	< 0.0001
Biopsy eosinophil, #/mm <sup>2</sup>	0.39 $\pm$ 1.28	13.40 $\pm$ 13.27	< 0.0001
Blood eosinophil, / $\mu$ L	109.3 $\pm$ 27.35	391.2 $\pm$ 47.15	0.0021
FeNO, ppb	20.05 $\pm$ 13.51	92.43 $\pm$ 59.40	< 0.0001

Values are presented as mean  $\pm$  SD

FEV<sub>1</sub>, forced expiratory volume in the first second. PD<sub>20</sub> provocative dosage required to cause a 20% decline in FEV<sub>1</sub>. The minimal and maximal provocative dosages were 0.01 and 2.505 mg, respectively. FeNO fraction of exhaled nitric oxide

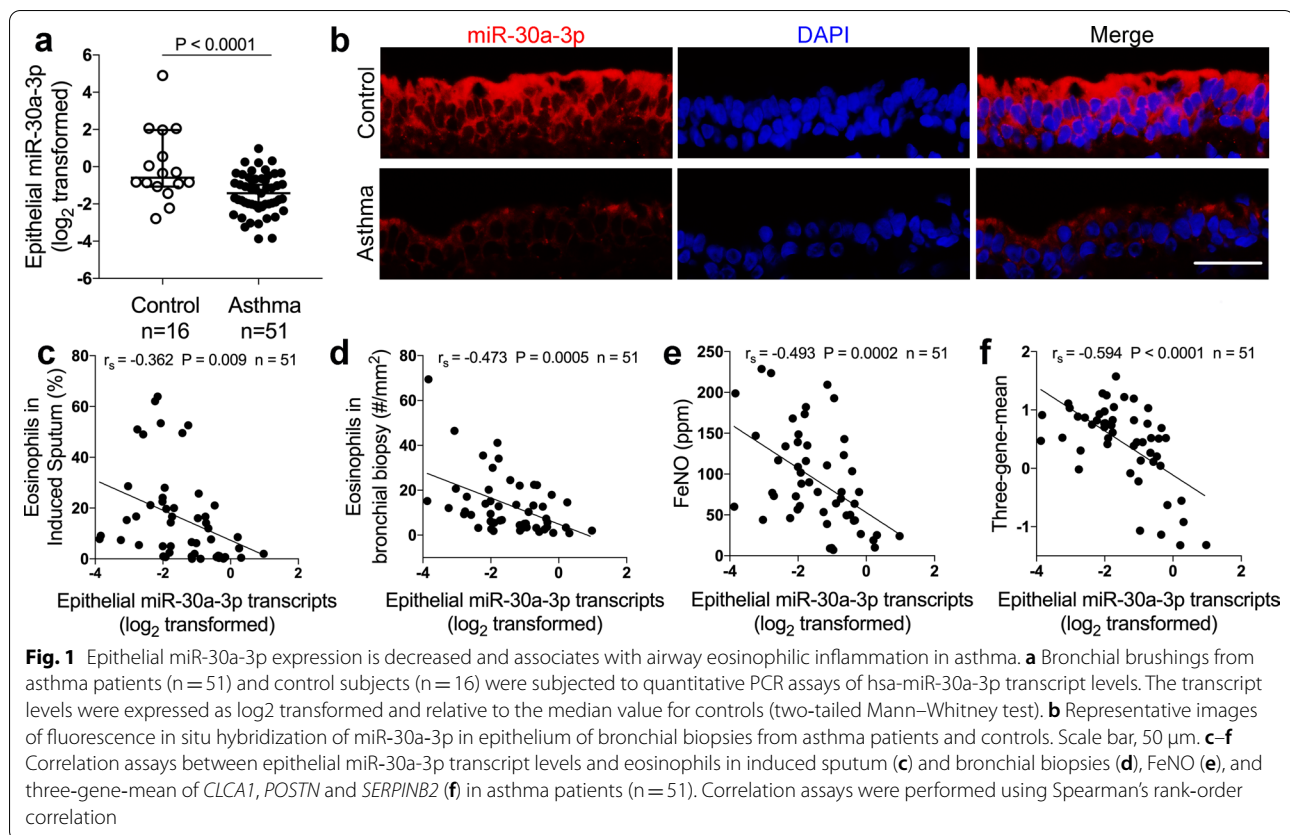
and used non-parametric tests (Mann–Whitney test or Kruskal–Wallis test with Dunn intergroup comparison). We analyzed correlations using Spearman's rank order correlation. Values of  $P < 0.05$  were considered statistically significant.

## Results

### Epithelial miR-30a-3p expression is decreased and associates with airway eosinophilic inflammation in asthma

Subject characteristics are summarized in Table 1. We measured the expression of miR-30a-3p in endobronchial brushing samples from treatment-naïve asthma patients ( $n = 51$ ) compared to control subjects ( $n = 16$ ) using quantitative PCR. We found that miR-30a-3p expression was significantly decreased in bronchial brushings in asthma patients compared with controls (Fig. 1a). Using fluorescent in situ hybridization, we demonstrated that miR-30a-3p was mainly located in the cytoplasm of airway epithelial cells (Fig. 1b).

Airway eosinophilic inflammation is a key feature of type 2-high asthma [1]. We found that miR-30a-3p had a strong negative correlation with parameters reflecting airway eosinophilia including eosinophil in induced sputum (Fig. 1c) and bronchial biopsies (Fig. 1d), and fraction of exhaled nitric oxide (Fig. 1e) in asthma patients. Furthermore, by measuring the expression of three epithelial signature genes (*CLCA1*, *POSTN*, *SERPINB2*) for type 2 status in endobronchial brushings using quantitative PCR [31], and by combination of these measurements to calculate a three-gene-mean for each subject,



we found that epithelial miR-30a-3p expression negatively correlated with three-gene-mean (Fig. 1f). Our data indicate that epithelial miR-30a-3p expression associates with the type 2 status in asthma. Thus, epithelial miR-30a-3p may play a role in airway eosinophilic inflammation in type 2-high asthma.

### **RUNX2 is a target of miR-30a-3p**

We predicted the candidate target genes of miR-30a-3p by using online algorithms including miRanda and TargetScan. *RUNX2* is one of the candidate target genes predicted by both online algorithms (Additional file 1: Table S2). The seed sequence of miR-30a-3p matches the 3'-untranslated region (UTR) of *RUNX2* (Fig. 2a). Co-transfection with the vector harboring wild-type *RUNX2* 3'-UTR and miR-30a-3p mimic decreased the luciferase activity. However, co-transfection with the vector containing mutant 3'-UTR or empty vector and miR-30a-3p mimic had no effect on the luciferase activity (Fig. 2b). This indicates that miR-30a-3p can directly bind to the 3'-UTR of *RUNX2*.

We used IL-13, a type 2 cytokine, to stimulate BEAS-2B bronchial epithelial cells. IL-13 decreased miR-30a-3p expression, but increased *RUNX2* expression in BEAS-2B cells (Fig. 2c, d). When transfection with

miR-30a-3p mimic, IL-13-induced *RUNX2* mRNA and protein expression were significantly decreased (Fig. 2g, i, j). In contrast, IL-13-induced *RUNX2* mRNA and protein expression were further enhanced when transfection with miR-30a-3p inhibitor (Fig. 2h, k, l). Our data suggest that *RUNX2* is a target of miR-30a-3p.

### **Epithelial RUNX2 is up-regulated and correlates with airway eosinophilia in asthma**

We found that *RUNX2* transcript levels were significantly increased in bronchial brushings from asthma patients when compared with controls (Fig. 3a). In support of *RUNX2* as a target of miR-30a-3p, epithelial *RUNX2* transcripts negatively correlated with miR-30a-3p expression in asthma patients (Fig. 3b). We next analyze the correlation between epithelial *RUNX2* expression and airway eosinophilia. Epithelial *RUNX2* transcript levels positively correlated with eosinophils in induced sputum (Fig. 3c) and bronchial biopsies (Fig. 3d), FeNO (Fig. 3e), and the three-gene-mean (Fig. 3f). This indicates that *RUNX2* may be involved in the pathogenesis of airway eosinophilic inflammation.

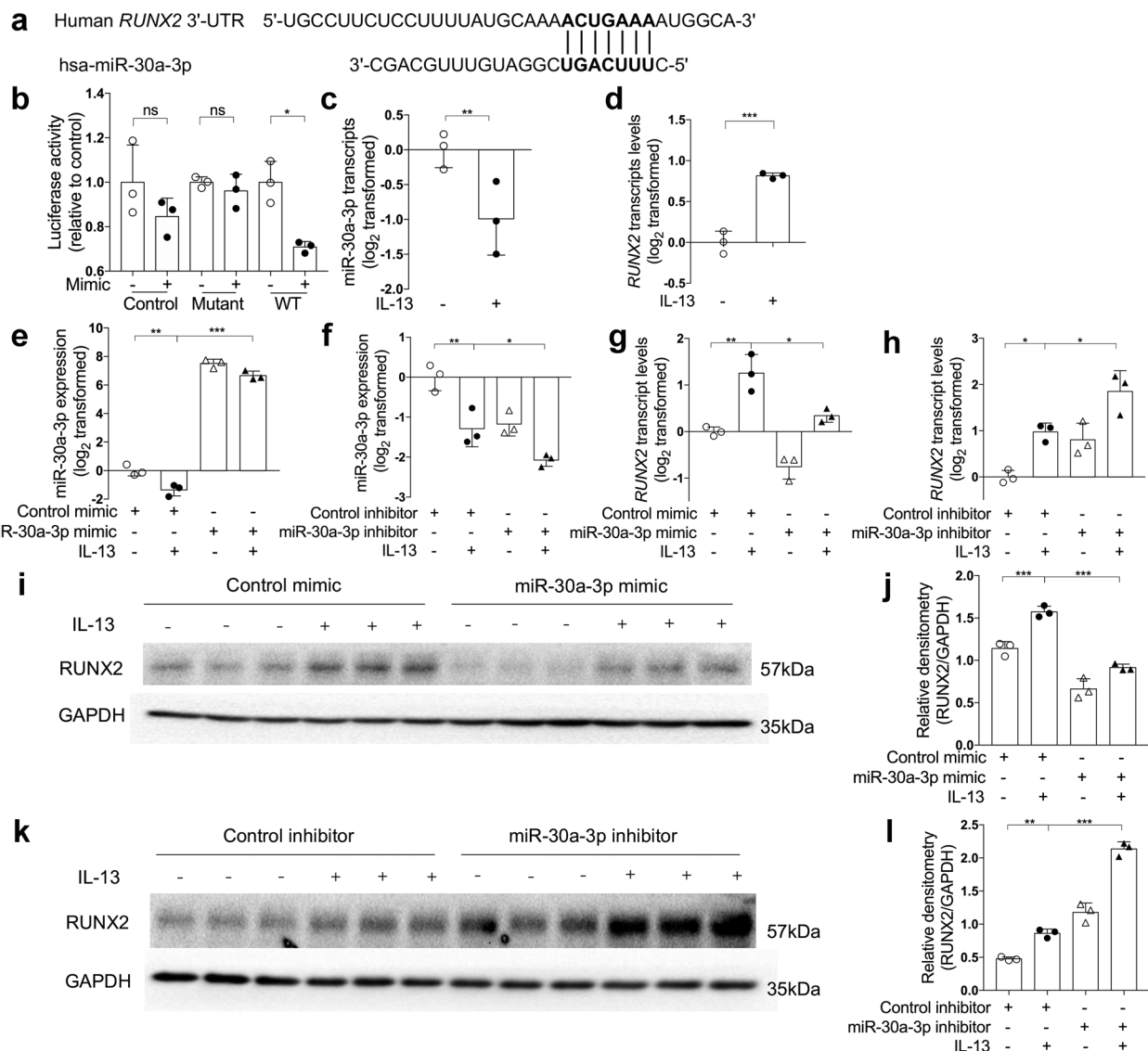
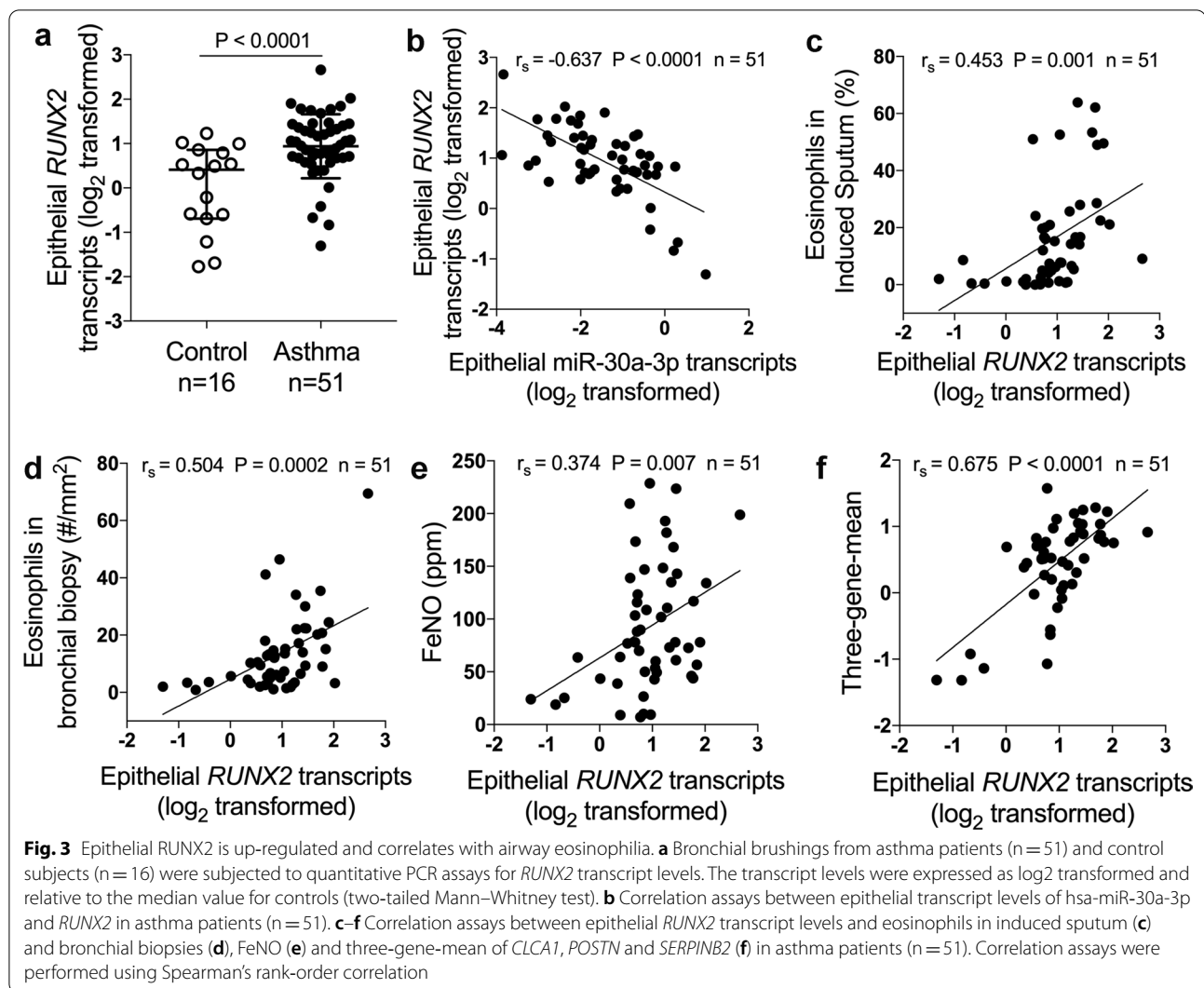


**Fig. 2** *RUNX2* is a target of miR-30a-3p. **a** The 3'-UTR of *RUNX2* contains the region matching the seed sequence of hsa-miR-30a-3p. **b** 3'-UTR luciferase reporter assay with vector harboring wild-type (WT), mutant *RUNX2* 3'-UTR or no 3'-UTR (control) co-transfected with miR-30a-3p mimic or control mimic, respectively. Luciferase activity was measured by dual-luciferase reporter assay system. The firefly luciferase activity was normalized to renilla luciferase activity. **c, d** The transcript levels of baseline and IL-13-induced miR-30a-3p (**c**) and *RUNX2* (**d**) in BEAS-2B cells were determined by quantitative PCR. The transcript levels were expressed as log<sub>2</sub> transformed and relative to the mean of control group (two-tailed Student's *t* test). **e, f** After control or miR-30a-3p mimic transfection with or without IL-13 stimulation, the transcript levels of miR-30a-3p were determined by quantitative PCR. **g, h** The transcript levels of *RUNX2*, after miR-30a-3p mimic (**g**) or inhibitor (**h**) transfection with or without IL-13 stimulation, were determined by quantitative PCR. The transcript levels were expressed as log<sub>2</sub> transformed and relative to the mean of control group (one-way ANOVA followed by Tukey's multiple comparison test). **i-l** The protein level of RUNX2 in BEAS-2B cells were determined by Western blotting after miR-30a-3p mimic (**i, j**) or inhibitor (**k, l**) transfection with or without IL-13 stimulation. Densitometry assay of the Western blotting results was analyzed using ImageJ, and the protein levels of RUNX2 were indexed to GAPDH. n = 3 wells per group. Data are mean ± SD. \*P < 0.05; \*\*P < 0.01; \*\*\*P < 0.001 (one-way ANOVA followed by Tukey's multiple comparison test)

### RUNX2 binds to the promoter of *HMGB1*

*HMGB1* plays a key role in the pathogenesis of airway inflammation in asthma [26]. According to a previous ChIP-on-chip analysis of *RUNX2* [21], *RUNX2* may bind to *HMGB1* gene. We predict the binding site of *RUNX2*

for *HMGB1* gene using JASPR (<http://jaspar.genereg.net/>) and found that *HMGB1* promoter DNA sequence, -1308 to -857 bp upstream of the *HMGB1* transcription start site, contains a 9-bp putative binding sequence for *RUNX2* (Fig. 4a). Using ChIP-PCR analysis, we



confirmed that RUNX2 directly binds to *HMGB1* promoter. Moreover, IL-13 treatment significantly enhanced the interaction between RUNX2 and HMGB1 compared to control cells (Fig. 4b).

To explore whether there are multiple binding sites for RUNX2 in the promoter region of *HMGB1*, luciferase reporters containing the wild type, truncated, or mutant *HMGB1* promoters were constructed (Fig. 4c). The luciferase activity of the reporter containing wild type *HMGB1* promoter was increased after co-transfection with RUNX2 cDNA plasmid. Of the four luciferase reporters containing mutant *HMGB1* promoter, luciferase activity was only increased in the mutant HMGB1 promoter containing the 9-bp binding sequence (−1098 to −1106 bp). Furthermore, mutation of the 9-bp binding sequence is sufficient to abrogate the increase of luciferase activity (Fig. 4d). This suggests that the *HMGB1* promoter regions contains a binding site for RUNX2.

#### RUNX2 promotes HMGB1 expression in airway epithelial cells

We next investigate whether RUNX2 promotes HMGB1 expression in airway epithelial cells. *HMGB1* transcript levels in bronchial brushings were significantly up-regulated in asthma patients compared to control subjects (Fig. 4e). Moreover, epithelial *RUNX2* transcript levels in bronchial brushings were positively correlated with *HMGB1* transcript levels in asthma patients (Fig. 4f). Immunofluorescent staining of bronchial biopsies revealed that the expression of RUNX2 and HMGB1 were both increased in the epithelial cells of asthma patients compared to controls (Fig. 4g). These data from asthma patients suggest that RUNX2 may contribute to HMGB1 expression in airway epithelial cells.

We further examined HMGB1 expression after RUNX2 knockdown or overexpression in BEAS-2B cells. Similar to *RUNX2*, the expression of *HMGB1* was increased after

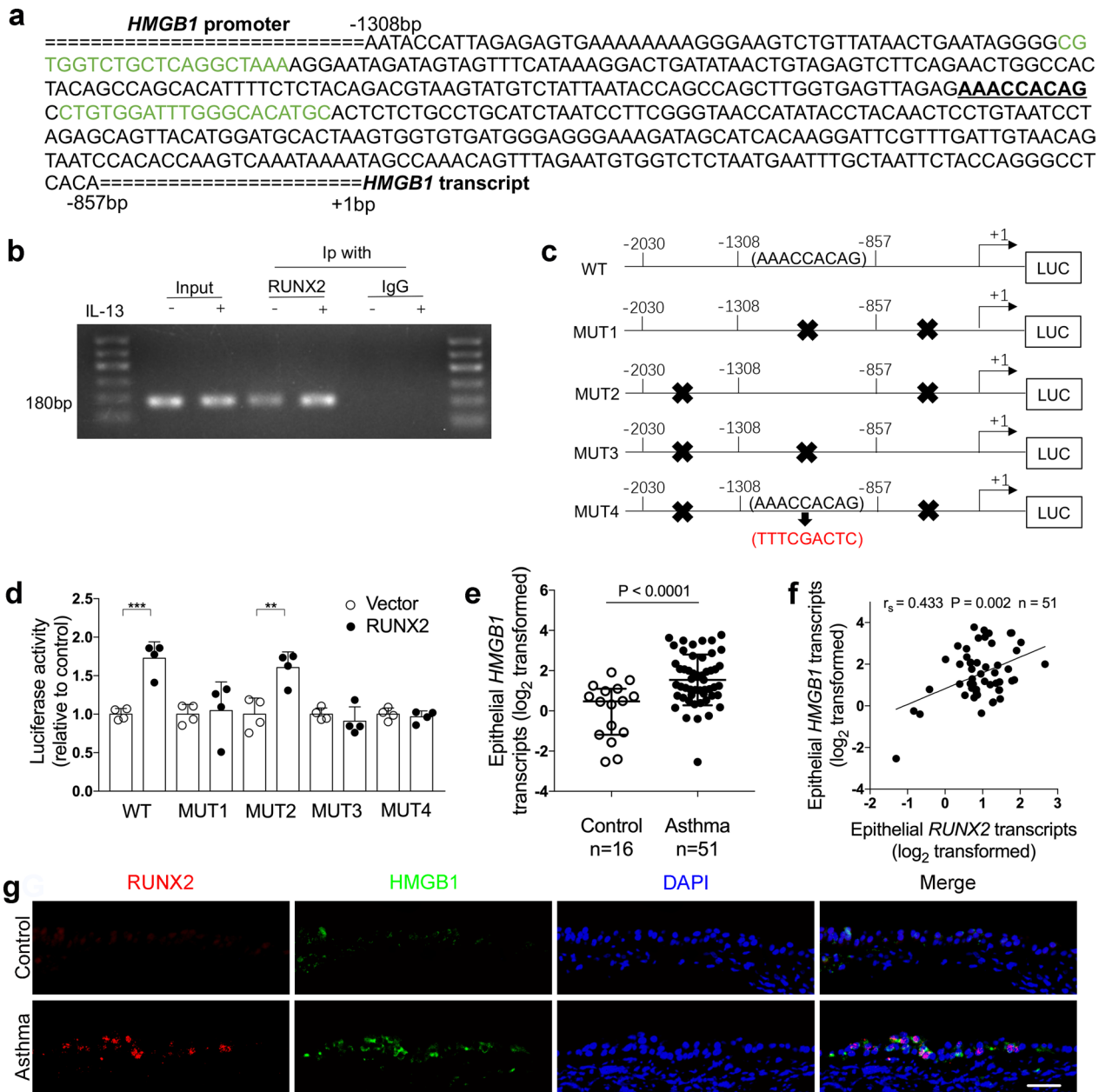


**Fig. 4** RUNX2 binds to the promoter of *HMGB1*. **a** The promoter region of *HMGB1* has a putative binding site for RUNX2. Sequence scheme of *HMGB1* promoter region with the putative RUNX2 binding element underlined (AAACCACAG). Sequences marked in green are primers for ChIP-PCR assay in panel B. **b** ChIP-PCR assays to amplify the 180-bp region of *HMGB1* promoter were performed to show direct binding of RUNX2 to *HMGB1* promoter in BEAS-2B cells. **c** Schematic presentation showing the luciferase reporter plasmid containing the wild type (WT), truncated, or mutant *HMGB1* promoter (MUT1–MUT4). MUT1 retains –2030 to –1308 bp, MUT2 retains –1308 to –857 bp, MUT3 retains –857 to +1 bp. MUT4 retains –1308 to –857 bp and the putative RUNX2 binding element AAACCACAG was replaced with TTTCGACTC. **d** The luciferase reporter plasmids containing WT and mutant *HMGB1* promoter were co-transfected with empty or RUNX2 cDNA expression vector. Luciferase activity was measured by dual-luciferase reporter assay system. The renilla luciferase activity was normalized to firefly luciferase activity (one-way ANOVA followed by Tukey’s multiple comparison test). n = 4 wells per group. Data are mean ± SD. \*P < 0.05; \*\*P < 0.01; \*\*\*P < 0.001. **e** *HMGB1* mRNA levels in bronchial brushings from asthma patients (n = 51) and controls (n = 16) were determined by quantitative PCR assays. The mRNA levels were expressed as log<sub>2</sub> transformed and relative to the median value of controls (two-tailed Mann–Whitney test). **f** Correlation assays between epithelial transcript levels of *RUNX2* and *HMGB1* in asthma patients (n = 51). Correlation assays were performed using Spearman’s rank-order correlation. **g** Representative images of RUNX2 (red) and *HMGB1* (green) immunofluorescence staining in bronchial biopsies from controls and asthma patients. Nuclei were stained with DAPI (blue). Scale bar, 50 μm



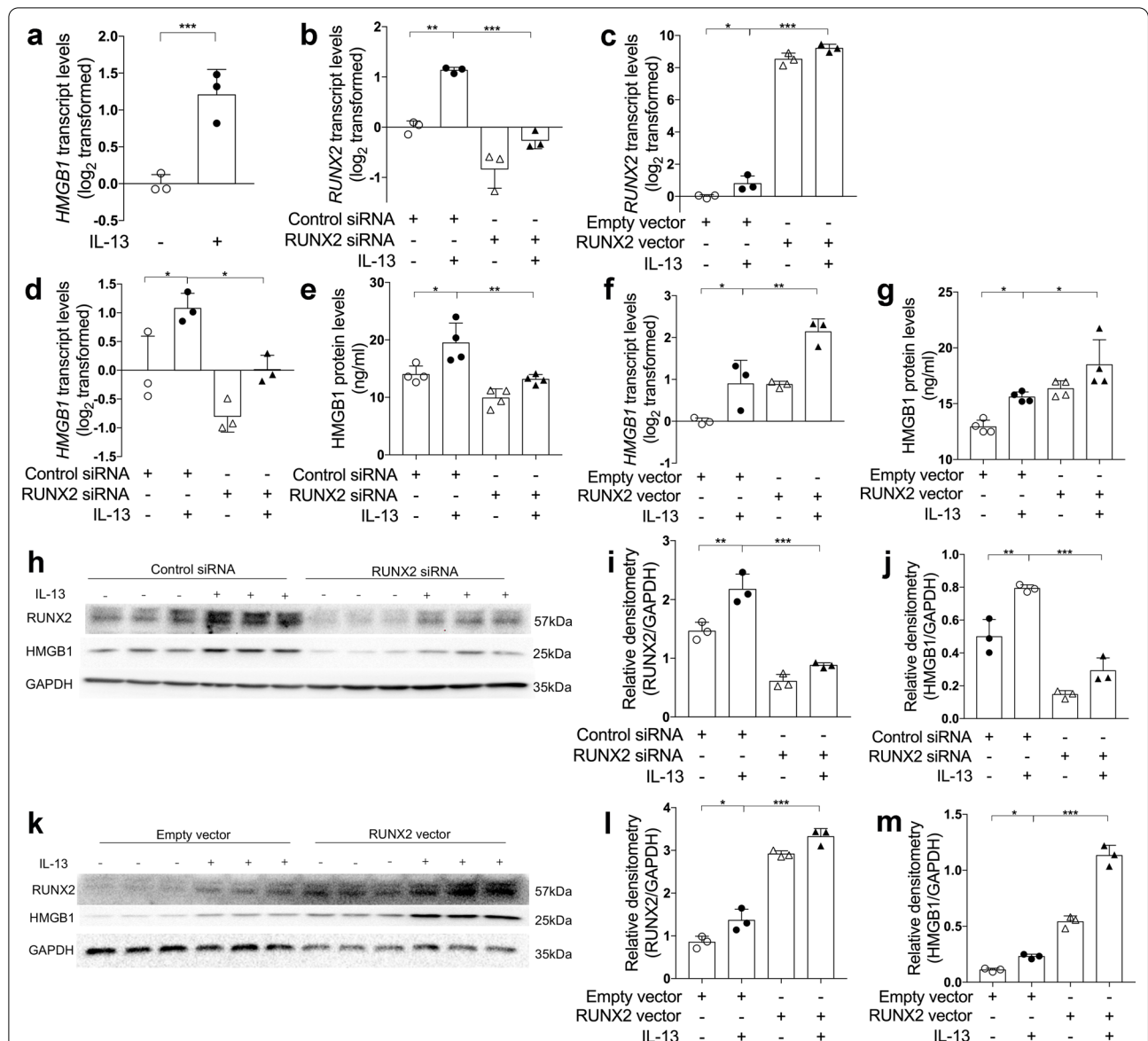


**Fig. 5** RUNX2 promotes HMGB1 expression in airway epithelial cells. **a** The transcript levels of miR-30a-3p in control and IL-13-stimulated BEAS-2B cells were determined by quantitative PCR. The transcript levels were expressed as log<sub>2</sub> transformed and relative to the mean of control group (two-tailed Student's *t* test). **b–d, f** The transcript levels of *RUNX2* (**b, c**) and *HMGB1* (**d, f**) after transfection with control or RUNX2 siRNA with or without IL-13 stimulation, and empty or RUNX2 cDNA expression vector with or without IL-13 stimulation were detected by quantitative PCR. The transcript levels were expressed as log<sub>2</sub> transformed and relative to the mean of control group. **e, g** The protein levels of HMGB1 in cell culture media were determined by ELISA, after transfection with control or RUNX2 siRNA (**e**) with or without IL-13 stimulation, and empty or RUNX2 cDNA expression vector (**g**) with or without IL-13 stimulation. **h–m** The protein levels of RUNX2 and HMGB1 in BEAS-2B were determined by Western blotting after transfection with control or RUNX2 siRNA with or without IL-13 stimulation (**h–j**), and empty or RUNX2 cDNA expression vector with or without IL-13 stimulation (**k–m**). Densitometry assay of the Western blotting results was analyzed using ImageJ, and the protein levels of RUNX2 and HMGB1 were indexed to GAPDH. *n* = 3–4 wells per group. Data are mean ± SD. \**P* < 0.05; \*\**P* < 0.01; \*\*\**P* < 0.001 (one-way ANOVA followed by Tukey's multiple comparison test)

IL-13 stimulation (Fig. 5a). RUNX2 knockdown by transfecting with siRNA against RUNX2 decreased IL-13-induced HMGB1 expression in BEAS-2B cells compared to the cells transfected with non-targeting control siRNA (Fig. 5b, d, e, h–j). In contrast, RUNX2 overexpression

by transfecting with a RUNX2 cDNA expression vector enhanced IL-13-induced HMGB1 expression compared with the cells transfected with empty vector (Fig. 5c, f, g, k–m). Our data indicate that RUNX2 promotes the expression of HMGB1 in airway epithelial cells.

In addition, we found that miR-30a-3p transcripts levels negatively correlated with *HMGB1* transcripts in bronchial brushings from asthma patients (Additional file 1: Fig. S1a). In BEAS-2B cells, miR-30a-3p overexpression by transfecting with miR-30a-3p mimic suppressed baseline and IL-13-induced *HMGB1* mRNA and protein expression. In contrast, transfection with miR-30a-3p inhibitor enhanced IL-13-induced *HMGB1* expression (Additional file 1: Fig. S1b–e). Together, our data suggest miR-30a-3p inhibits *HMGB1* expression by targeting *RUNX2*.

#### **Airway overexpression of mmu-miR-30a-3p suppresses airway eosinophilia in a murine model of allergic airway inflammation**

We further explored the role of miR-30a-3p in asthma using a murine model of allergic airway inflammation. Mice were sensitized and challenged with OVA, mmu-miR-30a-3p or control agomir was administered intranasally 2 h before OVA challenge on days 21, 23 (Fig. 6a). Compared with control mice, we found that the expression of mmu-miR-30a-3p was decreased in OVA-challenged mice using quantitative PCR and fluorescence in situ hybridization. MiR-30a-3p agomir administration significantly increased airway miR-30a expression (Fig. 6b, Additional file 1: Fig. S2). OVA sensitization and challenge resulted in infiltration of inflammatory cells around the airways as assessed using H&E staining and airway inflammation scoring (Fig. 6c, d). However, mmu-miR-30a-3p overexpression suppressed airway inflammation in OVA-challenged mice (Fig. 6c, d). Moreover, BALF cell counting revealed that mmu-miR-30a-3p overexpression decreased the number of eosinophils in BALF from OVA-challenged mice (Fig. 6e). This suggests that miR-30a-3p protects against airway eosinophilia in mouse asthma model. The transcript levels of *Ccl11* and *Ccl24* were both increased in lung tissue of OVA-challenged mice, but airway overexpression of miR-30a-3p did not suppress *Ccl11* and *Ccl24* expression (Additional file 1: Fig. S3). This indicates that miR-30a-3p may not affect the expression of eosinophil specific chemokines.

MiR-30a-3p is conserved across species, and the seed sequence of mmu-miR-30a-3p matches the 3'-UTR of *Runx2* (Fig. 7a). Using quantitative PCR and ELISA, we found that expression of *Runx2* and *Hmgb1* was markedly increased in OVA-challenge mice compared with control mice. However, airway overexpression of miR-30a-3p suppressed *Runx2* and *Hmgb1* expression (Fig. 7b–d). This supports our in vitro findings that miR-30a-3p targets *RUNX2*, and *RUNX2* promotes *HMGB1* expression. In addition, miR-30a-3p overexpression decreased the number of mucus cells and *Muc5ac* mRNA expression in OVA-challenged mice as assessed by PAS

staining and quantitative PCR, respectively (Additional file 1: Fig. S4). Since *RUNX2* was reported to regulate the differentiation of goblet cells, our data suggests that miR-30a-3p may suppress mucus overproduction by targeting *RUNX2*.

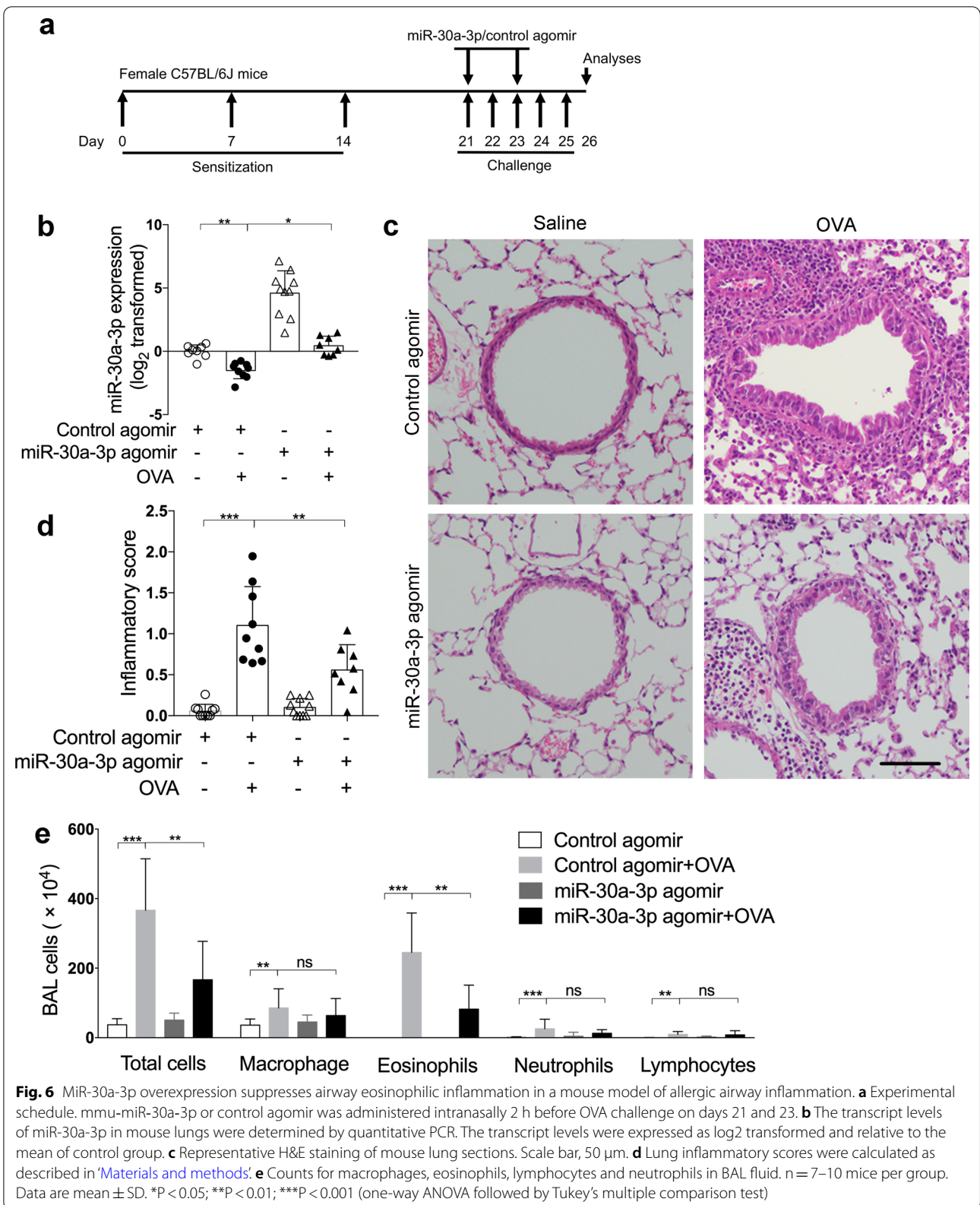
#### **Discussion**

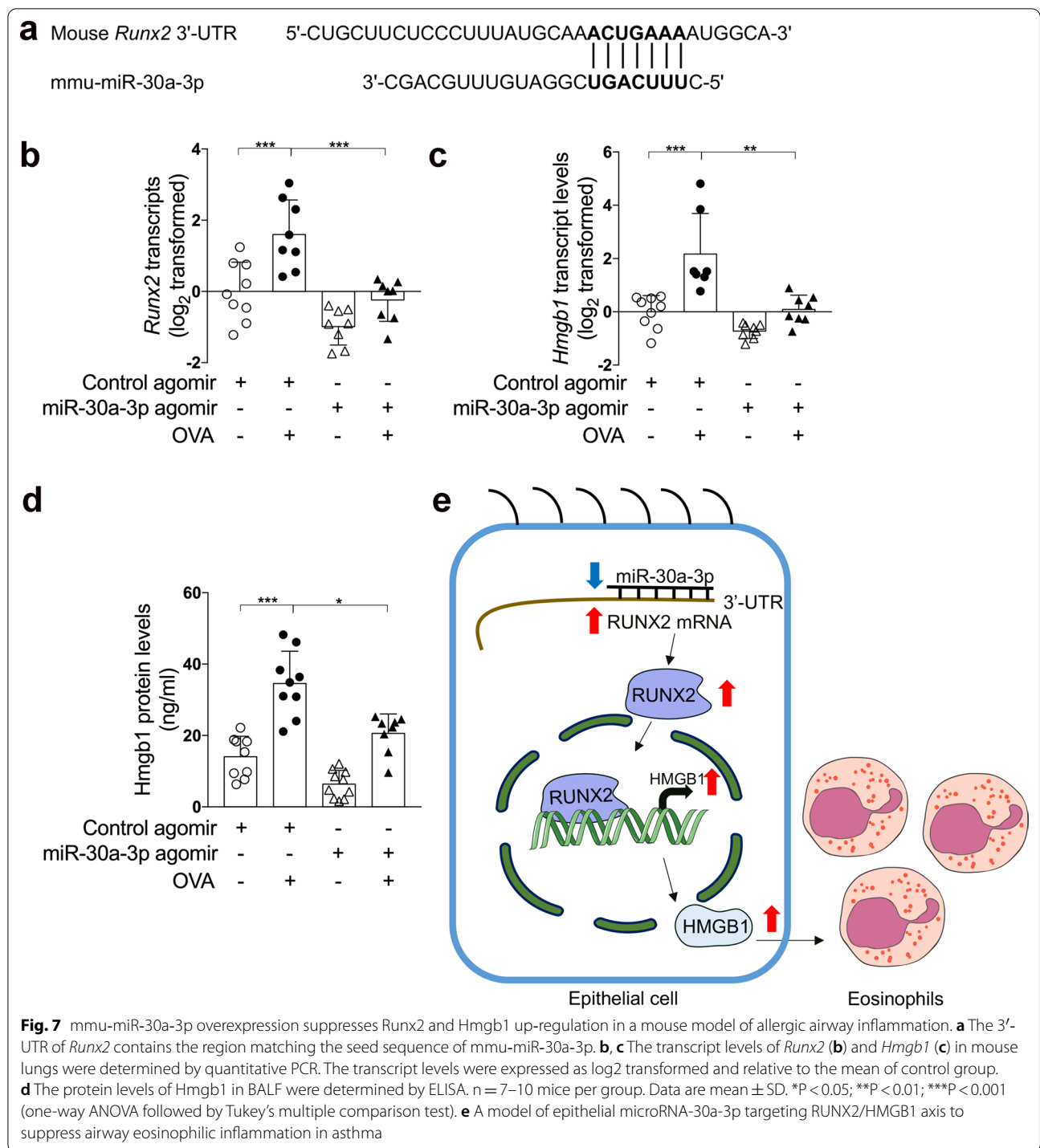
In the present study, we reported that miR-30a-3p expression was downregulated in bronchial epithelium in treatment-naïve asthma patients, in IL-13-stimulated human bronchial epithelial cells, and in the airways of a murine model of allergic airway inflammation. Moreover, epithelial miR-30a-3p expression was significantly correlated with airway eosinophilia in asthma patients. Our findings are consistent with the report that miR-30a-3p expression was decreased in the peripheral blood of asthmatic patients [15].

MiRNAs regulate gene expression by binding to the seed sequence in the 3'-UTR of target gene. We verified that *RUNX2* is a target gene of miR-30a-3p. *RUNX2* expression was significantly increased in bronchial epithelium of asthma patients, IL-13-stimulated human bronchial epithelial cells and in OVA-challenged mice airways. It was reported that upregulation of *RUNX2* in vascular smooth muscle cells increases the expression of inflammatory cytokines and promotes infiltration of inflammatory cells [32]. Consistently, we found that epithelial *RUNX2* expression was positively correlated with airway eosinophilia in asthma. This suggests that miR-30a-3p may play a role in airway eosinophilia by targeting *RUNX2*.

*RUNX2* is a transcription factor and a previous report suggests that *RUNX2* may interact with *HMGB1* [21]. However, there was no reports providing direct evidence that *RUNX2* binds to *HMGB1* promoter and regulates its expression. In this study, we found that *RUNX2* directly binds to a 9-bp sequence in the promoter of *HMGB1* gene. IL-13 enhances the binding of *RUNX2* to the *HMGB1* promoter. In BEAS-2B cells, we showed that knockdown or overexpression of *RUNX2* inhibited or intensified IL-13-induced *HMGB1* expression, respectively.

*HMGB1* can interact with the receptors including RAGE, TLR2 and TLR4 [33, 34]. Activation of these receptors finally leads to the production of various pro-inflammatory cytokines [35, 36]. We demonstrated that, like *RUNX2*, *HMGB1* expression was increased in bronchial epithelium of asthma patients, IL-13-stimulated human bronchial epithelial cells and OVA-challenged mice airways. In support of the role miR-30a-3p/*RUNX2* in the regulation of *HMGB1* expression, epithelial *HMGB1* expression was negatively correlated with





epithelial miR-30a-3p expression, and positively correlated with epithelial RUNX2 expression.

RUNX2 can also bind to the promoter of secreted phosphoprotein 1 (SPP1) [37]. SPP1, also named as osteopontin, is reported to be involved in airway inflammation [12, 38]. Thus, RUNX2 may contribute to airway

inflammation through regulating *Spp1* expression in addition to promoting HMGB1 expression. Interestingly, RUNX2 also regulates the expression of SPDEF, a critical factor for goblet cell differentiation [20].

Furthermore, we demonstrated the airway overexpression of mmu-miR-30a-3p suppressed airway inflammation

in OVA-challenged mice. The sequence of mmu-miR-30a-3p is identical to hsa-miR-30a-3p, and the 3'-UTR of murine *Runx2* gene has binding sites for the seed sequence of miR-30a-3p. In support of *Runx2* as a target of miR-30a-3p and as a transcription factor to regulate *Hmgb1* expression, mmu-miR-30a-3p overexpression decreased *Runx2* and *Hmgb1* expression in OVA-challenged mice. Additionally, mmu-miR-30a-3p overexpression also decreased the number of mucus cells and the expression of *Muc5ac*. This is consistent with the report that *RUNX2* can regulate the differentiation of goblet cells [20].

Our study has several limitations. First, the disproportionate sample size of asthma patients (n = 51) subjects and control subjects (n = 16) may lead to analysis bias. We repeated the statistical analyses in 16 asthma patients randomly selected from the cohort of 51 asthma patients in comparison to the 16 control subjects, and the results were consistent with those shown in Fig. 1 (Additional file 1: Fig. S5). This suggests there was no significant bias. Second, because a miRNA can target multiple genes expression, we can't exclude the possibility that miR-30a-3p regulates airway inflammation by targeting genes other than *RUNX2*.

## Conclusion

We conclude that epithelial miR-30a-3p could possibly target *RUNX2*/*HMGB1* axis to suppress airway eosinophilic inflammation in asthma.

## Abbreviations

ChIP: Chromatin immunoprecipitation; *RUNX2*: *RUNX* family transcription factor 2; *HMGB1*: High mobility group box 1; AHR: Airway hyperresponsiveness; IL: Interleukin; CCL: C-C motif chemokine ligand; miRNA: MicroRNA; SPDEF: SAM pointed domain containing ETS transcription factor; TLR: Toll-like receptor; RAGE: Receptor for advanced glycation end products; PD<sub>20</sub>: Dosage of methacholine provoking a 20% fall; FEV<sub>1</sub>: Forced expiratory volume in the first second; FeNO: Fraction of exhaled nitric oxide; BALF: Bronchoalveolar lavage fluid; H&E: Hematoxylin and eosin; PAS: Periodic acid-Schiff; PVDF: Polyvinylidene difluoride; ELISA: Enzyme linked immunosorbent assay; SD: Standard deviation.

## Supplementary Information

The online version contains supplementary material available at <https://doi.org/10.1186/s12931-022-01933-x>.

**Additional file 1: Table S1.** Primers for quantitative PCR. **Table S2.** Candidate targets of miR-30a-3p predicted by online algorithms miRanda and TargetScan. **Figure S1.** Inhibition of miR-30a-3p enhances the expression of *HMGB1*. **Figure S2.** Mmu-miR-30a-3p agomir is sufficient to abrogate the decrease of the expression of mmu-miR-30a-3p in OVA-challenge mice. **Figure S3.** Mmu-miR-30a-3p overexpression did not affect *Ccl11* and *Ccl24* expression in mouse lung tissue. **Figure S4.** Mmu-miR-30a-3p overexpression decreased the mucus production in OVA sensitized and challenged mice. **Figure S5.** The expression of miR-30a-3p, *RUNX2*, *HMGB1*, and the correlation between miR-30a-3p and airway eosinophilia in 16 asthma patients randomly selected from the cohort of 51 asthma patients.

## Acknowledgements

We thank all the participants in this study; Xiaoling Rao, Mei Liu, and Meifang Shen for bronchoscopy support; and Wang Ni, Kun Zhang, and Shixin Chen for spirometry measurement.

## Authors' contributions

LY and GZ conceived and designed research; WW, JG, DC, GC, YF, CC and SC performed experiments; WW, JG, DC, GC, YF, and GZ analyzed data; WW, JG, DC, GC, YF, CC, SC, LY, and GZ interpreted results of experiments; WW and GZ prepared figures; WW and GZ drafted manuscript; WW, LY and GZ edited and revised manuscript. All authors read and approved the final manuscript.

## Funding

This work was supported by National Natural Science Foundation of China (Grant 82170036, 91742108, 81670019, 81800026), National Key Research and Development Program of China (2016YFC1304400).

## Availability of data and materials

All data generated or analyzed during this study are included in this published article and its Additional file 1.

## Declarations

### Ethics approval and consent to participate

This study was approved by the institutional ethics board of Tongji Hospital of Tongji Medical College of Huazhong University of Science and Technology.

### Consent for publication

Not applicable.

### Competing interests

The authors have no competing interests to declare.

### Author details

<sup>1</sup>Division of Respiratory and Critical Care Medicine, Department of Internal Medicine, Tongji Hospital, Tongji Medical College, Huazhong University of Science and Technology, Wuhan 430030, China. <sup>2</sup>Key Laboratory of Respiratory Diseases, National Health Commission of People's Republic of China, and National Clinical Research Center for Respiratory Diseases, Wuhan, China.

Received: 15 August 2021 Accepted: 17 January 2022

Published online: 29 January 2022

## References

- Papi A, Brightling C, Pedersen SE, Reddel HK. Asthma. *Lancet* (London, England). 2018;391:783–800.
- Fahy JV. Type 2 inflammation in asthma—present in most, absent in many. *Nat Rev Immunol*. 2015;15:57–65.
- Kulkarni NS, Hollins F, Sutcliffe A, Saunders R, Shah S, Siddiqui S, Gupta S, Haldar P, Green R, Pavord I, et al. Eosinophil protein in airway macrophages: a novel biomarker of eosinophilic inflammation in patients with asthma. *J Allergy Clin Immunol*. 2010. <https://doi.org/10.1016/j.jaci.2010.03.026>.
- Suzukawa M, Morita H, Nambu A, Arai K, Shimura E, Shibui A, Yamaguchi S, Suzukawa K, Nakanishi W, Oboki K, et al. Epithelial cell-derived IL-25, but not Th17 cell-derived IL-17 or IL-17F, is crucial for murine asthma. *J Immunol* (Baltimore, Md: 1950). 2012;189:3641–52.
- Soumelis V, Reche PA, Kanzler H, Yuan W, Edward G, Homey B, Gilliet M, Ho S, Antonenko S, Lauerma A, et al. Human epithelial cells trigger dendritic cell mediated allergic inflammation by producing TSLP. *Nat Immunol*. 2002;3:673–80.
- Lai Y, Altemeier WA, Vandree J, Piliponsky AM, Johnson B, Appel CL, Frevert CW, Hyde DM, Ziegler SF, Smith DE, et al. Increased density of intraepithelial mast cells in patients with exercise-induced bronchoconstriction regulated through epithelially derived thymic stromal lymphopoietin and IL-33. *J Allergy Clin Immunol*. 2014;133:1448–55.

7. Siddiqui S, Johansson K, Joo A, Bonser LR, Koh KD, Le Tonqueze O, Bouchouchi S, Bautista RA, Zlock L, Roth TL, et al. Epithelial miR-141 regulates IL-13-induced airway mucus production. *JCI Insight*. 2021;6(5):e139019.
8. Bartel S, Carraro G, Alessandrini F, Krauss-Etschmann S, Ricciardolo FLM, Bellusci S. miR-142-3p is associated with aberrant WNT signaling during airway remodeling in asthma. *Am J Physiol Lung Cell Mol Physiol*. 2018;315:L328–33.
9. Pua HH, Happ HC, Gray CJ, Mar DJ, Chiou NT, Hesse LE, Ansel KM. Increased hematopoietic extracellular RNAs and vesicles in the lung during allergic airway responses. *Cell Rep*. 2019;26:933–944 e934.
10. Zhang K, Liang Y, Feng Y, Wu W, Zhang H, He J, Hu Q, Zhao J, Xu Y, Liu Z, Zhen G. Decreased epithelial and sputum miR-221-3p associates with airway eosinophilic inflammation and CXCL17 expression in asthma. *Am J Physiol Lung Cell Mol Physiol*. 2018;315:L253–64.
11. Liang Y, Feng Y, Wu W, Chang C, Chen D, Chen S, Zhen G. microRNA-218-5p plays a protective role in eosinophilic airway inflammation via targeting  $\delta$ -catenin, a novel catenin in asthma. *Clin Exp Allergy*. 2020;50:29–40.
12. Huo X, Zhang K, Yi L, Mo Y, Liang Y, Zhao J, Zhang Z, Xu Y, Zhen G. Decreased epithelial and plasma miR-181b-5p expression associates with airway eosinophilic inflammation in asthma. *Clin Exp Allergy*. 2016;46:1281–90.
13. Niu Z-R, Han T, Sun X-L, Luan L-X, Gou W-L, Zhu X-M. MicroRNA-30a-3p is overexpressed in the placentas of patients with preeclampsia and affects trophoblast invasion and apoptosis by its effects on IGF-1. *Am J Obstet Gynecol*. 2018. <https://doi.org/10.1016/j.ajog.2017.11.568>.
14. Wang Y, Wang F, He J, Du J, Zhang H, Shi H, Chen Y, Wei Y, Xue W, Yan J, et al. miR-30a-3p targets MAD2L1 and regulates proliferation of gastric cancer cells. *OncoTargets Ther*. 2019;12:11313–24.
15. Li X, Wang B, Huang M, Wang X. miR-30a-3p participates in the development of asthma by targeting CCR3. *Open Med (Wars)*. 2020;15:483–91.
16. Ito Y, Bae S-C, Chuang LSH. The RUNX family: developmental regulators in cancer. *Nat Rev Cancer*. 2015;15:81–95.
17. Coffman JA. Runx transcription factors and the developmental balance between cell proliferation and differentiation. *Cell Biol Int*. 2003;27:315–24.
18. Vimalraj S, Arumugam B, Miranda PJ, Selvamurugan N. Runx2: structure, function, and phosphorylation in osteoblast differentiation. *Int J Biol Macromol*. 2015;78:202–8.
19. Haley KJ, Lasky-Su J, Manoli SE, Smith LA, Shahsafaee A, Weiss ST, Tantisira K. RUNX transcription factors: association with pediatric asthma and modulated by maternal smoking. *Am J Physiol Lung Cell Mol Physiol*. 2011;301:L693–701.
20. Shi N, Zhang J, Chen S-Y. Runx2, a novel regulator for goblet cell differentiation and asthma development. *FASEB J*. 2017;31:412–20.
21. van der Deen M, Akech J, Lapointe D, Gupta S, Young DW, Montecino MA, Galindo M, Lian JB, Stein JL, Stein GS, van Wijnen AJ. Genomic promoter occupancy of runt-related transcription factor RUNX2 in Osteosarcoma cells identifies genes involved in cell adhesion and motility. *J Biol Chem*. 2012;287:4503–17.
22. Harris HE, Raucci A. Alarmin(g) news about danger: workshop on innate danger signals and HMGB1. *EMBO Rep*. 2006;7:774–8.
23. Sims GP, Rowe DC, Rietdijk ST, Herbst R, Coyle AJ. HMGB1 and RAGE in inflammation and cancer. *Annu Rev Immunol*. 2010;28:367–88.
24. Stenfeldt A-L, Wennerås C. Danger signals derived from stressed and necrotic epithelial cells activate human eosinophils. *Immunology*. 2004;112:605–14.
25. Lotfi R, Herzog GI, DeMarco RA, Beer-Stolz D, Lee JJ, Rubartelli A, Schrezenmeier H, Lotze MT. Eosinophils oxidize damage-associated molecular pattern molecules derived from stressed cells. *J Immunol (Baltimore, Md: 1950)*. 2009;183:5023–31.
26. Shim EJ, Chun E, Lee HS, Bang BR, Kim TW, Cho SH, Min KU, Park HW. The role of high-mobility group box-1 (HMGB1) in the pathogenesis of asthma. *Clin Exp*. 2012;42:958–65.
27. Hou C, Kong J, Liang Y, Huang H, Wen H, Zheng X, Wu L, Chen Y. HMGB1 contributes to allergen-induced airway remodeling in a murine model of chronic asthma by modulating airway inflammation and activating lung fibroblasts. *Cell Mol Immunol*. 2015;12:409–23.
28. Cheng D, Xue Z, Yi L, Shi H, Zhang K, Huo X, Bonser LR, Zhao J, Xu Y, Erle DJ, Zhen G. Epithelial interleukin-25 is a key mediator in Th2-high, corticosteroid-responsive asthma. *Am J Respir Crit Care Med*. 2014;190:639–48.
29. Myou S, Leff AR, Myo S, Boetticher E, Tong J, Meliton AY, Liu J, Munoz NM, Zhu X. Blockade of inflammation and airway hyperresponsiveness in immune-sensitized mice by dominant-negative phosphoinositide 3-kinase-TAT. *J Exp Med*. 2003;198:1573–82.
30. Livak KJ, Schmittgen TD. Analysis of relative gene expression data using real-time quantitative PCR and the 2(-Delta Delta C(T)) Method. *Methods*. 2001;25:402–8.
31. Woodruff PG, Boushey HA, Dolganov GM, Barker CS, Yang YH, Donnelly S, Ellwanger A, Sidhu SS, Dao-Pick TP, Pantoja C, et al. Genome-wide profiling identifies epithelial cell genes associated with asthma and with treatment response to corticosteroids. *Proc Natl Acad Sci USA*. 2007;104:15858–63.
32. Chen Y, Zhao X, Wu H. Transcriptional programming in arteriosclerotic disease: a multifaceted function of the Runx2 (runt-related transcription factor 2). *Arterioscler Thromb Vasc Biol*. 2021;41:20–34.
33. Zhu X, Cong J, Yang B, Sun Y. Association analysis of high-mobility group box-1 protein 1 (HMGB1)/toll-like receptor (TLR) 4 with nasal interleukins in allergic rhinitis patients. *Cytokine*. 2020;126:154880.
34. Feng X, Yang R, Tian Y, Miao X, Guo H, Gao F, Yang L, Zhao S, Zhang W, Liu J, et al. HMGB1 protein promotes glomerular mesangial matrix deposition via TLR2 in lupus nephritis. *J Cell Physiol*. 2020;235:5111–9.
35. Zenerino C, Nuzzo AM, Giuffrida D, Biolcati M, Zicari A, Todros T, Rolfo A. The HMGB1/RAGE pro-inflammatory axis in the human placenta: modulating effect of low molecular weight heparin. *Molecules (Basel, Switzerland)*. 2017;22(11):1997.
36. Cheng Y, Wang D, Wang B, Li H, Xiong J, Xu S, Chen Q, Tao K, Yang X, Zhu Y, He S. HMGB1 translocation and release mediate cigarette smoke-induced pulmonary inflammation in mice through a TLR4/MyD88-dependent signaling pathway. *Mol Biol Cell*. 2017;28:201–9.
37. Komori T. Regulation of bone development and extracellular matrix protein genes by RUNX2. *Cell Tissue Res*. 2010;339:189–95.
38. Barreno RX, Richards JB, Schneider DJ, Cromar KR, Nadas AJ, Hernandez CB, Hallberg LM, Price RE, Hashmi SS, Blackburn MR, et al. Endogenous osteopontin promotes ozone-induced neutrophil recruitment to the lungs and airway hyperresponsiveness to methacholine. *Am J Physiol Lung Cell Mol Physiol*. 2013;305:L118–129.

## Publisher's Note

Springer Nature remains neutral with regard to jurisdictional claims in published maps and institutional affiliations.

Ready to submit your research? Choose BMC and benefit from:

- fast, convenient online submission
- thorough peer review by experienced researchers in your field
- rapid publication on acceptance
- support for research data, including large and complex data types
- gold Open Access which fosters wider collaboration and increased citations
- maximum visibility for your research: over 100M website views per year

At BMC, research is always in progress.

Learn more [biomedcentral.com/submissions](https://biomedcentral.com/submissions)

